

Manganese-Catalyzed Cycloalkene Ring Expansion Synthesis of Azaheterocycles

Zhixin Wang, Hanxiao Xu, Xuanzhen Han, Shuaixin Fan, and Jin Zhu*

Department of Polymer Science and Engineering, School of Chemistry and Chemical Engineering, State Key Laboratory of Coordination Chemistry, Nanjing University, Nanjing 210023, China.

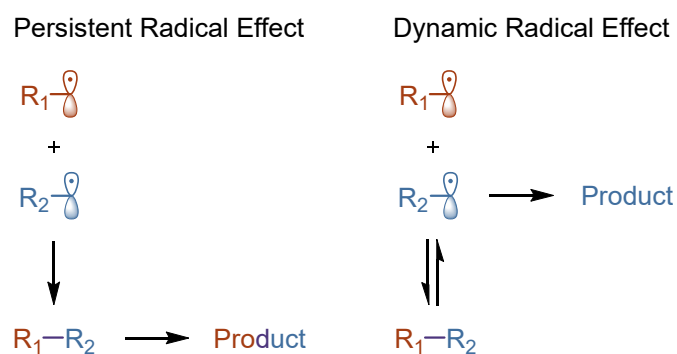
*Corresponding author. Email: jinz@nju.edu.cn.

Abstract: Radical chemistry is synthetically useful but can be plagued by the non-intuitive reaction course and indiscriminate reactivity profile. Herein, dynamic radical effect is revealed as a conceptual logic for the predictive achievement of radical reaction selectivity. The reversible bonding association/dissociation of two radicals serves as a synthetic handle for directing one radical to the target reaction recourse, without the participation of the other radical. A Mn catalytic protocol has been developed for cycloalkene ring expansion synthesis of azaheterocycles. An initial azidyl radical addition to alkene and subsequent reversible O₂ occupation of C-radical site prevents further radical coupling and steers the reaction toward the intramolecular rearrangement pathway. A broad substrate scope has been established for the synthesis of pyridine and isoquinoline derivatives. This new radical synthetic perspective promises as an important guiding principle for empowering radical-based chemical transformations.

Keyword: Dynamic Radical Effect; Manganese Catalysis; Cycloalkene; Ring Expansion; Azaheterocycle.

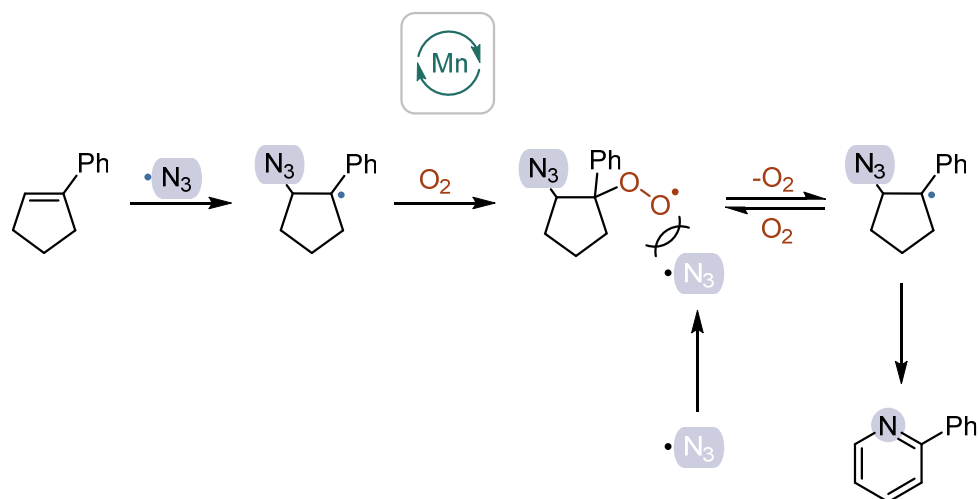
Radical reactions are chemical transformations that involve the participation of open-shell species with unpaired electrons.¹ This mode of reaction chemistry has emerged as an important tool for organic synthesis, in many ways complementary to the polar counterpart.² Despite the synthetic utility, a major drawback associated with radical chemistry is, frequently, its non-intuitive reaction course and indiscriminate reactivity profile. To address the issue, extensive experimental efforts have been directed at the mechanistic understanding of reaction pathway and rational achievement of reaction selectivity.³ A representative conceptual advance of broad impact is persistent radical effect (Scheme 1), a proposition devised to account for and for access to the synthetically valuable high cross-selectivity of radical bonding association event.⁴ Two radicals, when differing significantly in lifetimes, with one termed as a transient radical (short lifetime) and the other termed as a persistent radical (long lifetime), can undergo effective cross-coupling with each other to afford target product. This is a strikingly discriminative reaction course that can be predominant (e.g., at the stationary state) over other alternative pathways. Indeed, persistent radical effect has been repeatedly observed in radical processes and a hallmark of those processes is the locked-in bonding affiliation of persistent radical, irrespective of the intermediate reaction course of transient radical (e.g., atom transfer radical addition and atom transfer radical polymerization reactions).⁵ Herein we wish to disclose the discovery of dynamic radical effect (Scheme 1), in reference to a phenomenon that the bonding association between two radicals (e.g., a transient radical and a persistent radical) is reversible and upon bonding dissociation, one radical (e.g., the transient radical)

Scheme 1. Persistent Radical Effect and Dynamic Radical Effect.



proceeds to the target reaction course without the participation of other radical (e.g., the persistent radical).⁶ In particular, a Mn-catalyzed cycloalkene ring expansion transformation has been achieved for the synthesis of azaheterocycles (Scheme 2): Initial azidyl radical addition to cycloalkene affords a transient C-centered radical; cross-coupling association with a persistent diradical O₂ to a peroxy radical blocks the C-radical site from second azidation; reversible dissociation of O₂ (low temperature favors association and disfavors dissociation; high temperature favors both association and dissociation) regenerates the C-radical; attack on the azido group extrudes N₂ and provides an aziridinyl radical; intramolecular rearrangement furnishes the azaheterocycle product.

Scheme 2. Mn-Catalyzed Cycloalkene Ring Expansion Transformation.



Radicals are high-energy species and reaction with an alkene typically progresses to the double addition state.⁷ For a *N*-centered azidyl radical (as well as other electrophilic radicals), double azidation has been routinely observed as an, essentially predestined, reaction end point.⁸ In this circumstance, typically no innate radical chain cycle is operative due to the inefficient azidyl transfer process (as in many atom transfer radical addition reactions) and transition metal catalysis is a requisite (with the second azidation designated as the radical-metal crossover reaction from the persistent radical effect formalism perspective).⁹ For the mono addition of a *N*-centered moiety, nitrene is generally the reactive species of choice. Although the nature of the electronic states (singlet or triplet) can be subject to debate under various scenarios (e.g., in different transition metal complexes), the valency deficiency ensures the exclusive single nitrene transfer reactivity.¹⁰ The dynamic radical effect as witnessed in the reversible association/dissociation of O₂, serving to temporarily occupy the transient radical site and competitively exclude the site from further radical coupling, offers a distinct mechanistic platform for the mono addition of a radical species. More importantly, it is expected that the dynamic radical effect might evolve into a generically applicable strategy for directing the radical reaction to a totally different transformation pathway. For example, the low-temperature association of O₂ and its high-temperature dissociation can be a prospective switch for the stepwise, as opposed to the conventional continuous, double radical addition to an alkene, with intermediate manipulation of the radical process possible.¹¹ In fact, the dynamic, reversible radical-radical, radical-neutral molecule bonding association/dissociation might be

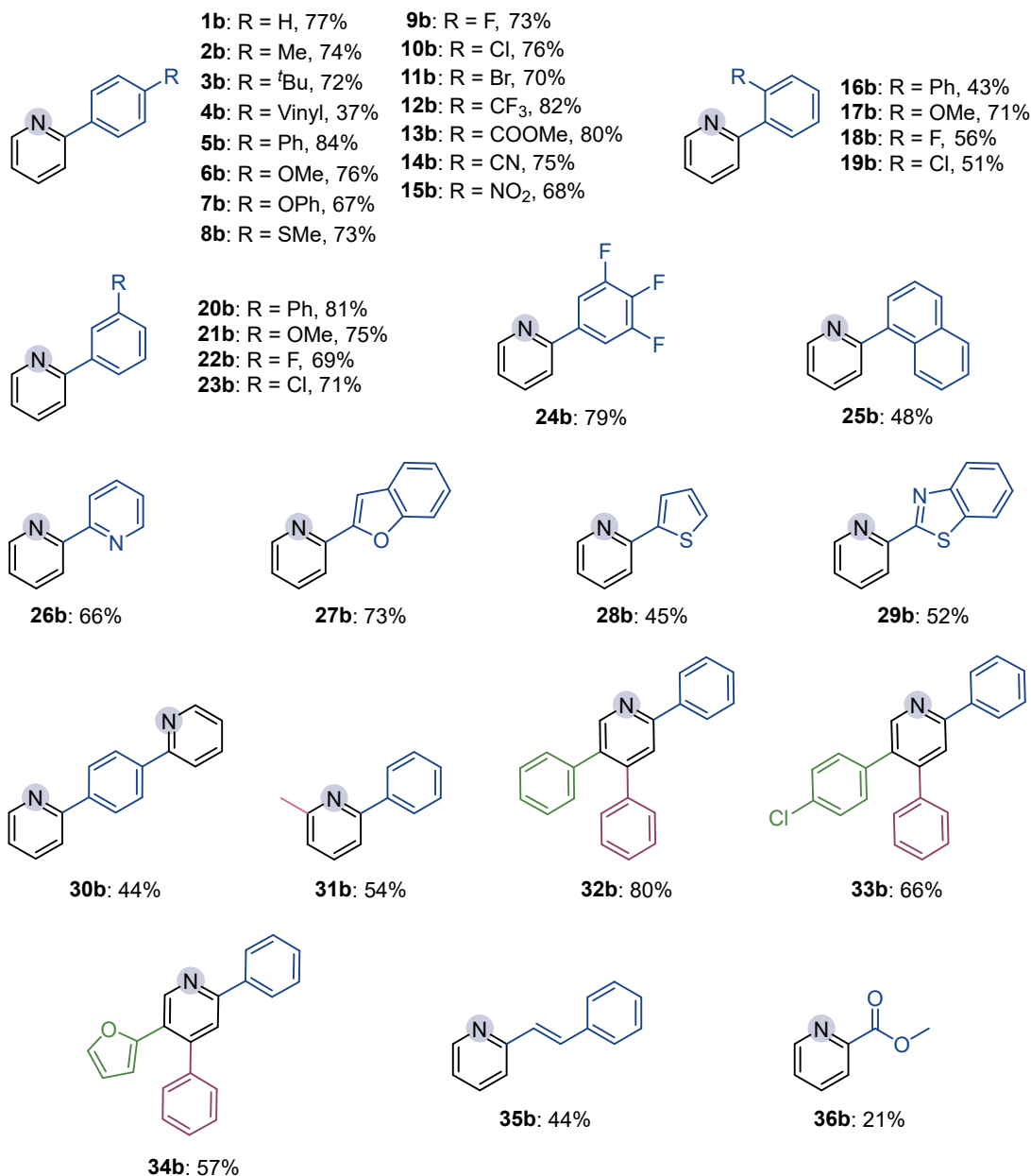
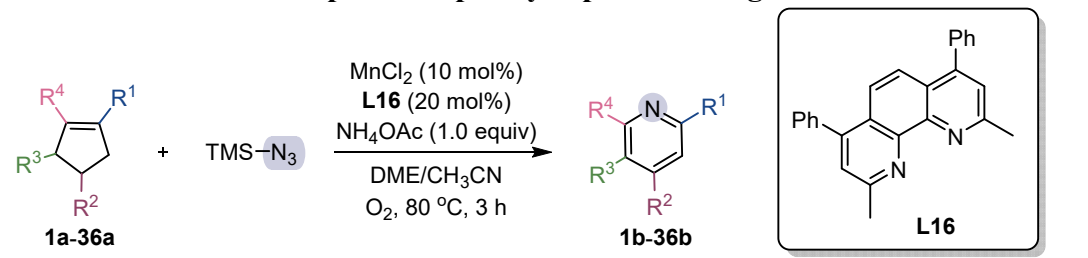
ubiquitously present in radical processes, setting dynamic radical effect as a unique thermodynamic/kinetic control handle for synthetic radical coupling reactions. As an added note, dynamic radical effect is distinct from radical-based catalysis (e.g., radical addition/elimination catalysis) as the latter implicates the full participation of radical catalyst throughout the catalytic cycle.

We commence our experimental inquiry into a Mn-catalyzed reaction between 1-phenylcyclopentene (**1a**) and TMSN₃ under the oxidative atmosphere of air. The selection of Mn catalysis is for two reasons: 1) transition metals in general can serve as versatile buffering sites for radical species, exhibiting a highly productive capture-release turnover efficiency; 2) Mn ranks third in abundance among transition metals and features rich redox properties.¹² The option for polar TMSN₃ (polar with respect to the Si-N bond, related to the redox potential) as the azide source is in view of its easy oxidative conversion to an azidyl radical; this contrasts with the less polar, PhSO₂N₃-like reagent (less polar with respect to the S-N bond), which typically reacts via a bimolecular homolytic substitution (S_H2) or nitrene pathway.¹³ Initial screening of reaction conditions identifies Mn(acac)₃ (10 mol%) as a viable catalyst precursor, with PPh₃ (20 mol%) as the ligand and NH₄OAc (1.0 equiv) as the additive, and 25% ring-expanded product 2-phenylpyridine (**1b**) can be obtained after 10 h of 80 °C reaction in dimethoxyethane (DME). The yield can be increased to 30% with a change to MnCl₂. With MnCl₂ fixed, extensive survey of ligands reveals a bidentate nitrogen-based ligand, **L16**, as the optimum choice, and a 62% yield can be reached. Further check into the solvents informs a yield of 71% in CH₃CN and a yield of 73% in DME/CH₃CN (2:1).

In DME/CH₃CN (2:1), with the oxidative atmosphere altered from air to O₂, the yield can be optimized to 77% for a shortened 3 h reaction.

With the reaction condition optimized and synthetic protocol developed, the simple-ring cycloalkene substrate scope is then examined (Scheme 3). A broad range of substitution patterns, both electron-donating and electron-withdrawing, on the phenyl ring of **1a** are compatible with the ring expansion transformation to pyridine derivatives.¹⁴ For the electron-donating *para* substitution, an alkyl group (Me, **2a**, 74%; *t*Bu, **3a**, 72%) largely maintains the product yield; the reactivity is drastically lower with the vinyl group (**4a**, 37%); the phenyl group (**5a**), in contrast, can elevate the yield to 84%; the OMe group (**6a**, 76%) provides a higher yield than the OPh group (**7a**, 67%); the swap of O with S offers a similar reactivity (SMe, **8a**, 73%). For the electron-withdrawing *para* substitution, the yield is generally preserved with a halide group (F, **9a**, 73%; Cl, **10a**, 76%; Br, **11a**, 70%); notably, the reactivity is also sustained with CF₃ (**12a**, 82%), COOMe (**13a**, 80%), CN (**14a**, 75%), and NO₂ (**15a**, 68%) groups. For the *ortho* substitution, likely due to the steric hindrance, the product yield (Ph, **16a**, 43%; OMe, **17a**, 71%; F, **18a**, 56%; Cl, **19a**, 51%) can be reduced to a varied degree as compared to the *para* counterpart. For the *meta* substitution, with the relaxation of steric hindrance (versus the *ortho* counterpart), the yield (Ph, **20a**, 81%; OMe, **21a**, 75%; F, **22a**, 69%; Cl, **23a**, 71%) is restored to the *para* counterpart level. The *meta, meta, para* trisubstitution (**24a**, 79%) is also compatible with the reaction. The replacement of phenyl in **1a** with 1-naphthyl (**25a**, 48%) results in a vast drop in the product yield. The replacement with a heterocyclic group (2-pyridyl, **26a**, 66%; 2-benzofuryl, **27a**, 73%;

Scheme 3. Substrate Scope of Simple Cyclopentene Rings.^{a,b}



^aReaction condition: **1a-36a** (0.2 mmol), TMSN_3 (0.5 mmol), MnCl_2 (10 mol%), NH_4OAc (1.0 equiv), **L16** (20 mol%), DME: CH_3CN =2:1 (2 mL), under O_2 , $80\text{ }^\circ\text{C}$, 3 h. ^bIsolated yields.

2-thiophenyl, **28a**, 45%; 2-benzothiazolyl, **29a**, 52%) shows a varied effect on the yield.

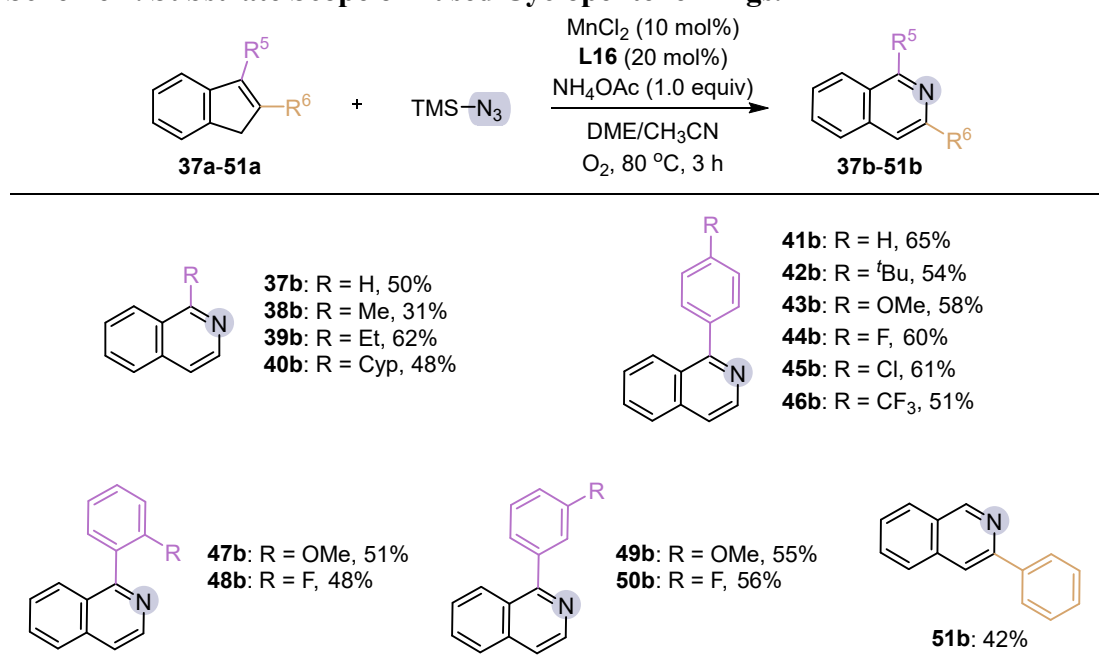
The extra *para* positioning of a second cyclopentene ring on **1a** (**30a**, 44%) offers a

double ring-expanded product. With the phenyl substitution scope explored and broad functional group tolerance verified, the cyclopentenyl substitution scope of **1a** is next investigated. Apparently both steric and electronic effects play a role in determining the reactivity: The yield is decreased to 54% with the 2-Me substitution (**31a**), whereas with the 3,4-diphenyl substitution (**32a**), an 80% yield can be acquired; with an extra *para* Cl group on the 3-phenyl of **32a** (**33a**), the yield is lowered to 66%, and the replacement of 3-phenyl of **32a** with 2-furyl (**34a**, 57%) also diminishes the yield. Satisfactorily, (*E*)-1-styrylcyclopentene (**35a**, 44%) and 1-methoxycarbonylcyclopentene (**36a**, 21%), with an alkenyl and an ester group (instead of a phenyl group as in **1a**) directly attached to the cyclopentene ring, are also viable substrates for the reaction.

With the simple cyclopentene ring substrate scope inspected, the scrutiny of fused cyclopentene ring scope is then executed (Scheme 4). The ring expansion of indene (**37a**) can progress to a 50% yield for the target product isoquinoline. The 3-Me (**38a**, 31%), 3-Et (**39a**, 62%), and 3-cyclopropyl (or 3-Cyp) (**40a**, 48%) substitutions show respectively a lower, a higher, and an intermediary yield. The yield reaches 65% with the 3-phenyl substitution (**41a**). An extra *para* substitution on the 3-phenyl group trims the yield to a varied extent depending on the substituent (*t*Bu, **42a**, 54%; OMe, **43a**, 58%; F, **44a**, 60%; Cl, **45a**, 61%; CF₃, **46a**, 51%). With the substitution at the *ortho* position (OMe, **47a**, 51%; F, **48a**, 48%), the yield goes down further. With the *meta* substitution (OMe, **49a**, 55%; F, **50a**, 56%), the yield rises back to the *para* counterpart level. The change of 3-phenyl substitution (as in **41a**) to the 2-phenyl substitution (**51a**)

slashes the yield to 42%.

Scheme 4. Substrate Scope of Fused Cyclopentene Rings.^{a,b}

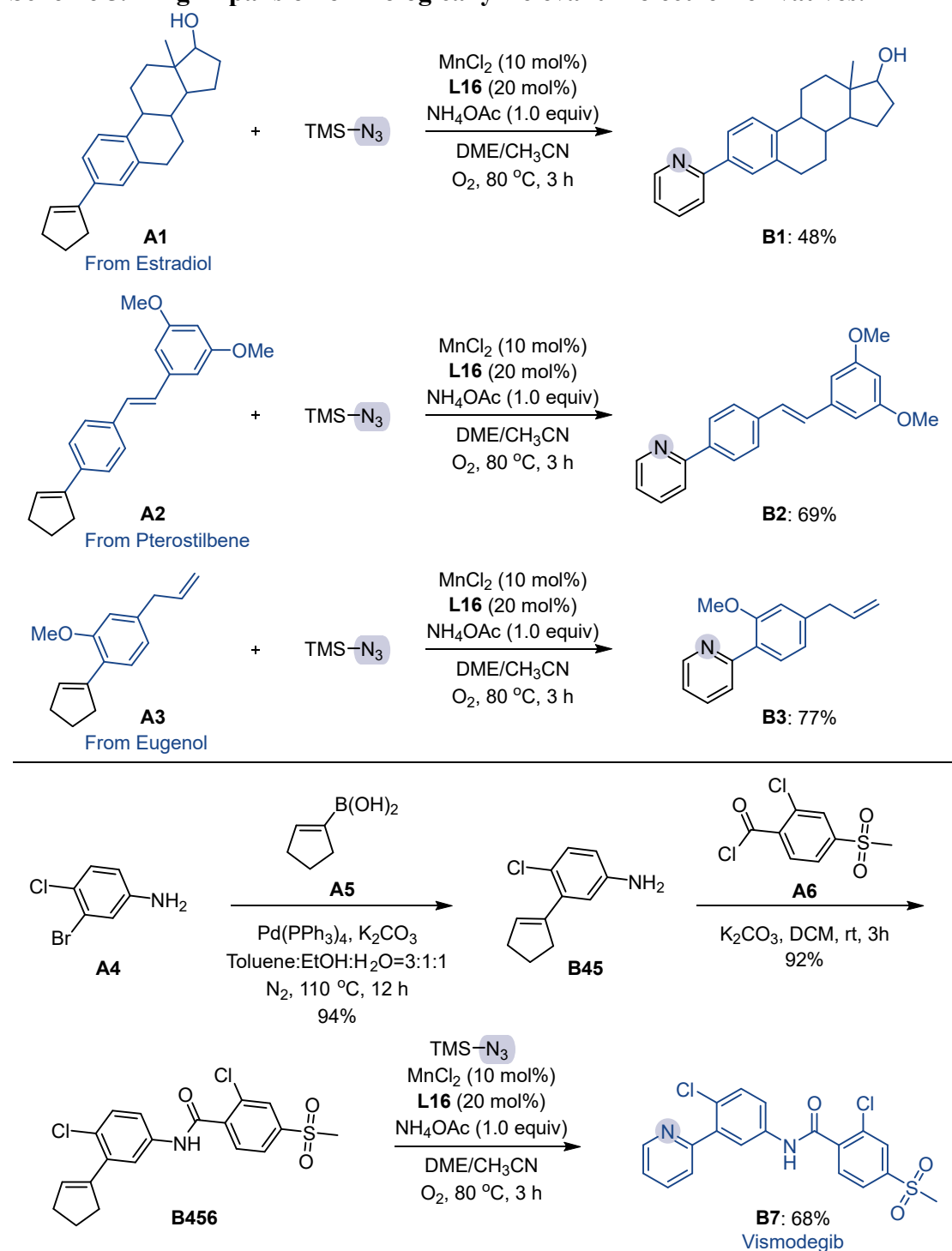


^aReaction condition: **37a-51a** (0.2 mmol), TMSN_3 (0.5 mmol), MnCl_2 (10 mol%), NH_4OAc (1.0 equiv), **L16** (20 mol%), DME: CH_3CN =2:1 (2 mL), under O_2 , 80 °C, 3 h. ^bIsolated yields.

With the substrate scope fully probed, protocol applications in various late-stage synthetic settings are pursued (Scheme 5). An estradiol-derived compound **A1** can be transformed to product **B1**, with the 1-cyclopentenyl-to-2-pyridyl correspondence ring expansion, at a 48% yield. Likewise, a pterostilbene-derived compound **A2** can be transformed to **B2** (69%); An eugenol-derived **A3** can be transformed to **B3** (77%). Noteworthy in these transformations is the tolerance of remote hydroxyl and alkene groups. The protocol competency in a multi-step synthesis scenario is exemplified with vismodegib (Scheme 5), a U.S. Food and Drug Administration-approved medication for the interfering of Hedgehog signaling pathway.¹⁵ A three-step procedure sequence of Suzuki coupling between **A4** and **A5** to **B45** (94%), amide bond formation between **B45** and **A6** to **B456** (92%), and ring expansion of **B456** to **B7** (vismodegib, 68%)

features an overall yield of 59%.

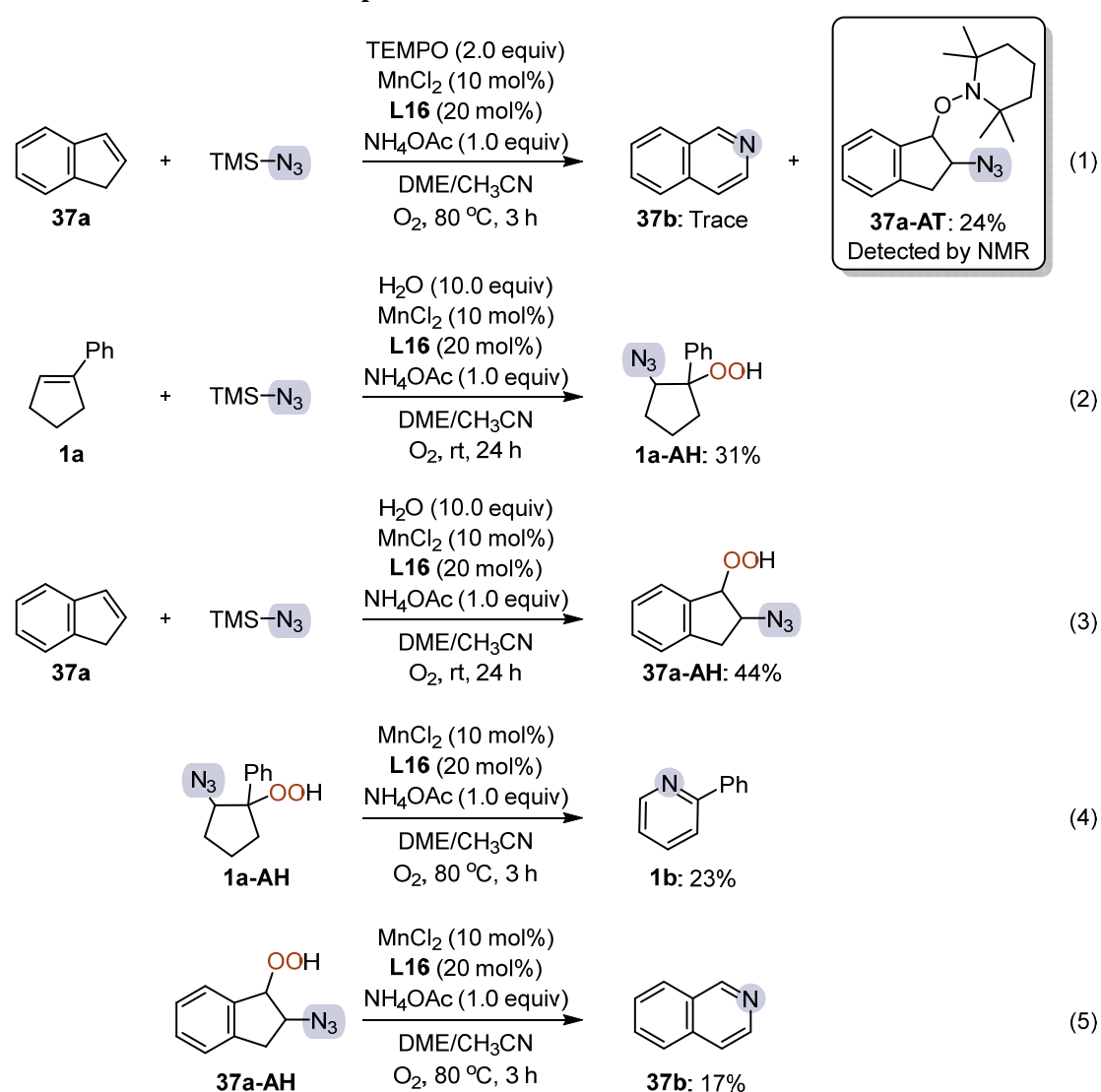
Scheme 5. Ring Expansion of Biologically Relevant Molecule Derivatives.



With the synthetic applications demonstrated, an experimental inquiry into the reaction mechanism is undertaken. Control experiments for the ring expansion transformation of **1a** suggest the required engagement of MnCl_2 , TMSN_3 , and O_2 (no

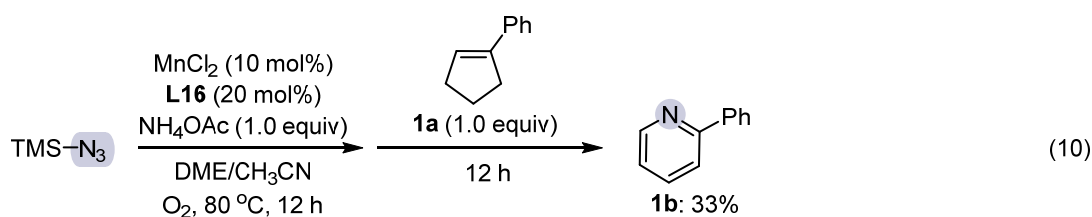
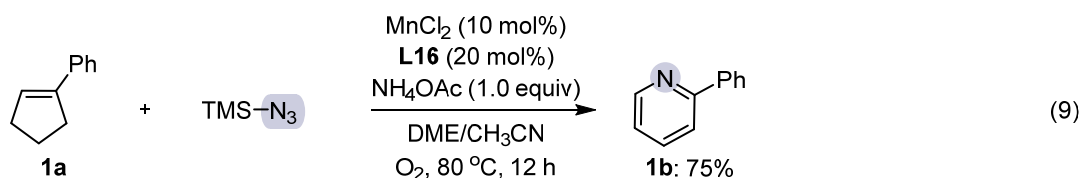
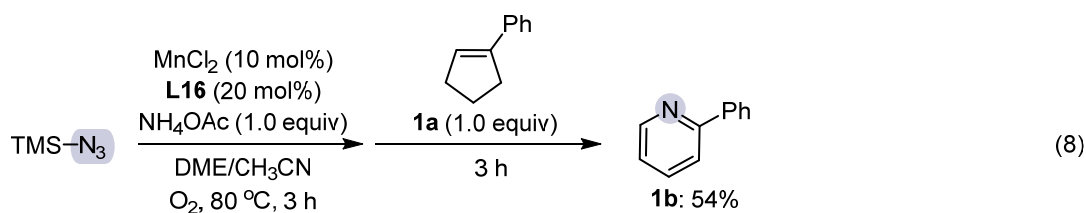
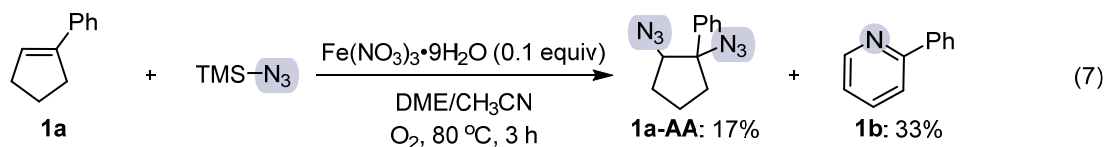
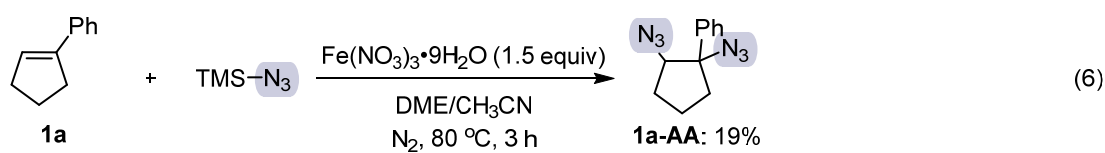
product detected without either one of three), beneficial effect of ligand **L16** (yield in absence: 39%) and NH₄OAc (yield in absence: 44%), and as a corollary, TMSN₃ as the nitrogen source in azaheterocycles. An initial hint at the radical, instead of the nitrene nature of the ring expansion process comes from three observations (Scheme 6): 1) the interception of a 2-azido-3-TEMPO (2,2,6,6-tetramethyl-1-piperidinyloxy) adduct of **37a**, **37a-AT** (24%), in the presence of TEMPO, 2) the regioselective site location of the azido group in **37a-AT**, 3) the virtually complete repression of ring expansion reaction course for **1a** and **37a** by both TEMPO and butylated hydroxytoluene (BHT). These observations advocate azidyl radical addition to cycloalkene as the ring expansion boot step. Apparently, O₂, together with **L16**-ligated Mn, is responsible for the oxidative azidyl radical generation. Following this mechanistic insight, a further meticulous room temperature (rt) (instead of 80 °C optimized condition) experiment for **1a** and **37a** allows the isolation of 2-azido-1-hydroperoxy adduct of **1a** (**1a-AH**, 31%) and 2-azido-3-hydroperoxy adduct of **37a** (**37a-AH**, 44%), respectively. This observation, albeit rt-based, reveals that O₂ can compete effectively against azidyl radical for bonding association with the C-radical. The mechanistic significance of O₂ bonding association for the ring expansion process herein is evidenced by the successful transformation of **1a-AH** and **37a-AH**, through extrusion of the hydroperoxy group, to the respective ring-expanded products (23% and 17% yield, respectively) under 80 °C optimized condition. The non-ideal yield can be attributed to the extra hydrogen atom affixed to the peroxy group, which is absent in the authentic ring expansion process. Collectively, these observations are consistent with the reversible association and

Scheme 6. Mechanistic Experiments I.



dissociation of O₂ in the ring expansion transformation. The dynamic radical effect, as showcased herein in the reversible association/dissociation of O₂, competitive temporary occupation of the C-radical site and exclusion from further radical coupling, has also been independently identified and corroborated in an Fe oxidative system (Scheme 7): without the dynamic radical effect, **1a** undergoes successive azidation to the diazidation product **1a-AA** (19%) at 80 °C under 1.5 equiv Fe(NO₃)₃·9H₂O and N₂; with the dynamic radical effect of O₂ interference, the competitive ring expansion transformation to target product (33%) can be observed under 10 mol%

Scheme 7. Mechanistic Experiments II.



Fe(NO₃)₃·9H₂O.^{9a} Last, a critical enabling factor for the emergence of dynamic radical effect is the slow release of azidyl radical for the maintenance of an appropriate concentration (diazidation can compete effectively at a high azidyl radical concentration) (Scheme 7). Indeed, the initial extended release of azidyl radical followed by the addition reaction with **1a** can still sustain the product formation (3 h-3 h sequence, 54%; 12 h reaction, 75%; 12 h-12 h sequence, 33%). Taken together, key mechanistic prerequisites for achieving the dynamic radical effect include: appropriate concentration of azidyl radical, favored competitive O₂ association/dissociation dynamics with C-radical over azidyl radical, and efficient and productive

intramolecular radical rearrangement.

In conclusion, a Mn catalytic protocol has been developed for cycloalkene ring expansion synthesis of azaheterocycles. A radical azidyl-derived process is operative for the broad-scope production of pyridine and isoquinoline derivatives. The dynamic radical effect, featuring the reversible association/dissociation of O₂ and competitive temporary occupation of transient radical site and exclusion from further radical coupling, directs the reaction toward the intramolecular ring expansion rearrangement pathway. This new conceptual perspective on the radical processes promises as an important general guiding principle for both the understanding and design of radical-empowered synthetic schemes.

References

- (1) (a) Bouwman, J.; McCabe, M. N.; Shingledecker, C. N.; Wandishin, J.; Jarvis, V.; Reusch, E.; Hemberger, P.; Bodi, A. Five-membered ring compounds from the *ortho*-benzyne+methyl radical reaction under interstellar conditions. *Nat. Astron.* **2023**, *7*, 423-430. (b) Ruffoni, A.; Mykura, R. C.; Bietti, M.; Leonori, D. The interplay of polar effects in controlling the selectivity of radical reactions. *Nat. Synth.* **2022**, *1*, 682-695.
- (2) (a) Huang, H.-M.; Bellotti, P.; Ma, J.; Dalton, T.; Glorius, F. Bifunctional reagents in organic synthesis. *Nat. Rev. Chem.* **2021**, *5*, 301-321. (b) Jiang, S.; Wang, W.; Mou, C.; Zou, J.; Jin, Z.; Hao, G.; Chi, Y. R. Facile access to benzofuran derivatives through radical reactions with heteroatom-centered super-electron-donors. *Nat. Commun.* **2023**, *14*, 7381. (c) Lee, W.-C.; Zhang, X. P. Metalloradical catalysis: general approach for controlling reactivity and selectivity of homolytic radical reactions. *Angew. Chem. Int. Ed.* **2024**, *63*, e202320243. (d) Matsuki, Y.; Ohnishi, N.; Kakeno, Y.; Takemoto, S.; Ishii, T.; Nagao, K.; Ohmiya, H. Aryl radical-mediated *N*-heterocyclic carbene catalysis. *Nat. Commun.* **2021**, *12*, 3848. (e) Jin, L.-M.; Xu, P.; Xie, J.; Zhang, X. P. Enantioselective intermolecular radical C-H amination. *J. Am. Chem. Soc.* **2020**, *142*, 20828-20836. (f) Wang, J.; Lu, H.; He, Y.; Jing, C.; Wei, H. Cobalt-catalyzed nitrogen atom insertion in arylcycloalkenes. *J. Am. Chem. Soc.* **2022**, *144*, 22433-22439.
- (3) (a) Zhang, M.; Ye, Z.; Zhao, W. Cobalt-catalyzed asymmetric remote borylation of alkyl halides. *Angew. Chem. Int. Ed.* **2023**, *62*, e202306248. (b) Mandal, T.; Das, S.; Maji, R.; De Sarkar, S. Visible-light-induced hydrogen atom transfer en route to exocyclic alkenylation of cyclic ethers enabled by electron donor-acceptor complex. *Org.*

Lett. **2023**, *25*, 7727-7732. (c) Wang, X.; Cui, P.; Xia, C.; Wu, L. Catalytic boration of alkyl halides with borane without hydrodehalogenation enabled by titanium catalyst. *Angew. Chem. Int. Ed.* **2021**, *60*, 12298-12303. (d) Jiang, Y.; Li, S.; Wang, S.; Zhang, Y.; Long, C.; Xie, J.; Fan, X.; Zhao, W.; Xu, P.; Fan, Y.; et al. Enabling specific photocatalytic methane oxidation by controlling free radical type. *J. Am. Chem. Soc.* **2023**, *145*, 2698-2707. (e) Zhou, W.; Su, H.; Cheng, W.; Li, Y.; Jiang, J.; Liu, M.; Yu, F.; Wang, W.; Wei, S.; Liu, Q. Regulating the scaling relationship for high catalytic kinetics and selectivity of the oxygen reduction reaction. *Nat. Commun.* **2022**, *13*, 6414. (f) Petroselli, M.; Rebek, J., Jr.; Yu, Y. Highly selective radical monoreduction of dihalides confined to a dynamic supramolecular host. *Chem. Eur. J.* **2021**, *27*, 3284-3287. (g) Mandal, M.; Buss, J. A.; Chen, S. J.; Cramer, C. J.; Stahl, S. S. Mechanistic insights into radical formation and functionalization in copper/*N*-fluorobenzenesulfonimide radical-relay reactions. *Chem. Sci. Trans.* **2024**, *15*, 1364-1373.

(4) (a) Roldan, B. J.; Hammerstad, T. A.; Galliher, M. S.; Keylor, M. H.; Pratt, D. A.; Stephenson, C. R. J. Leveraging the persistent radical effect in the synthesis of *trans*-2,3-diaryl dihydrobenzofurans. *Angew. Chem. Int. Ed.* **2023**, *62*, e202305801. (b) Ling, B.; Yao, S.; Ouyang, S.; Bai, H.; Zhai, X.; Zhu, C.; Li, W.; Xie, J. Nickel-catalyzed highly selective radical C-C coupling from carboxylic acids with photoredox catalysis. *Angew. Chem. Int. Ed.* **2024**, e202405866. (c) Patra, T.; Bellotti, P.; Strieth-Kalthoff, F.; Glorius, F. Photosensitized intermolecular carboimination of alkenes through the persistent radical effect. *Angew. Chem. Int. Ed.* **2020**, *59*, 3172-3177. (d) Simek, M.;

Bartova, K.; Pohl, R.; Cisarova, I.; Jahn, U. Tandem anionic oxy-cope rearrangement/oxygenation reactions as a versatile method for approaching diverse scaffolds. *Angew. Chem. Int. Ed.* **2020**, *59*, 6160-6165.

(5) (a) Ho, T. D.; Lee, B. J.; Tan, C.; Utley, J. A.; Ngo, N. Q.; Hull, K. L. Efficient synthesis of alpha-haloboronic esters via Cu-catalyzed atom transfer radical addition. *J. Am. Chem. Soc.* **2023**, *145*, 27230-27235. (b) Zhang, M.; Zhao, W.; Ma, J.; Li, J.; Meng, Q.; Shen, C.; Zeng, X. Syn-selective chlorosulfonylation of alkynes via a copper-powder-initiated atom transfer radical addition reaction and mechanistic studies. *Org. Lett.* **2023**, *25*, 231-235. (c) Cheng, X.-Y.; Zhang, Y.-F.; Wang, J.-H.; Gu, Q.-S.; Li, Z.-L.; Liu, X.-Y. A counterion/ligand-tuned chemo- and enantioselective copper-catalyzed intermolecular radical 1,2-carboamination of alkenes. *J. Am. Chem. Soc.* **2022**, *144*, 18081-18089. (d) Engl, S.; Reiser, O. Copper-photocatalyzed ATRA reactions: concepts, applications, and opportunities. *Chem. Soc. Rev.* **2022**, *51*, 5287-5299. (e) Sun, M.; Zhang, L.; Li, C. Modified cellulose nanocrystals based on SI-ATRP for enhancing interfacial compatibility and mechanical performance of biodegradable PLA/PBAT blend. *Polym. Compos.* **2022**, *43*, 3753-3764.

(6) (a) Liu, K.; Schwenger, M.; Studer, A. Radical NHC catalysis. *ACS Catal.* **2022**, *12*, 11984-11999. (b) Roldan, B. J.; Hammerstad, T. A.; Galliher, M. S.; Keylor, M. H.; Pratt, D. A.; Stephenson, C. R. J. Leveraging the persistent radical effect in the synthesis of *trans*-2,3-diaryl dihydrobenzofurans. *Angew. Chem. Int. Ed.* **2023**, *62*, e202305801.

(c) Morsdorf, J. M.; Ballmann, J. Coordination-induced radical generation: selective hydrogen atom abstraction via controlled Ti-C sigma-bond homolysis. *J. Am. Chem.*

Soc. **2023**, *145*, 23452-23460.

(7) (a) Li, K.; Deng, J.; Long, X.; Zhu, S. Photoinduced synthesis of C2-linked phosphine oxides via radical difunctionalization of acetylene. *Green Chem.* **2023**, *25*, 7253-7258. (b) Yang, B.; Lu, S.; Wang, Y.; Zhu, S. Diverse synthesis of C2-linked functionalized molecules via molecular glue strategy with acetylene. *Nat. Commun.* **2022**, *13*, 1858.

(8) Zheng, Y.-T.; Xu, H.-C. Electrochemical azidocyanation of alkenes. *Angew. Chem. Int. Ed.* **2024**, *63*, e202313273.

(9) (a) Zhang, M.; Zhang, J.; Li, Q.; Shi, Y. Iron-mediated ligand-to-metal charge transfer enables 1,2-diazidation of alkenes. *Nat. Commun.* **2022**, *13*, 7880. (b) Bian, K.-J.; Kao, S.-C.; Nemoto, D., Jr.; Chen, X.-W.; West, J. G. Photochemical diazidation of alkenes enabled by ligand-to-metal charge transfer and radical ligand transfer. *Nat. Commun.* **2022**, *13*, 7881.

(10) (a) Shen, Y. T.; Ran, Y.-S.; Jiang, B.; Zhang, C.; Jiang, W.; Li, Y.-M. Azido-difluoromethylthiolation of alkenes with TMSN₃ and PhSO₂SCF₂H. *Org. Lett.* **2023**, *25*, 4525-4529. (b) Chen, F.; Tang, Y.-T.; Li, X.-R.; Duan, Y.-Y.; Chen, C.-X.; Zheng, Y. Oxoammonium salt-mediated vicinal oxyazidation of alkenes with NaN₃: access to β -aminoxy azides. *Adv. Synth. Catal.* **2021**, *363*, 5079-5084.

(11) Kim, Y.; Bielawski, C. W.; Lee, E. Oxygen atom transfer: a mild and efficient method for generating iminyl radicals. *Chem. Commun.* **2019**, *55*, 7061-7064.

(12) (a) Ding, D.; Chen, X.; Su, X.; She, Y.-B.; Yang, Y.-F. Computational insights into the dual reactivity of 1,2,3,4-tetrazole: a metalloporphyrin-catalyzed click reaction and

denitrogenative annulation. *Org. Chem. Front.* **2023**, *10*, 5055-5063. (b) Li, F.; Long, L.; He, Y.-M.; Li, Z.; Chen, H.; Fan, Q.-H. Manganese-catalyzed asymmetric formal hydroamination of allylic alcohols: a remarkable macrocyclic ligand effect. *Angew. Chem. Int. Ed.* **2022**, *61*, e202202972. (c) Liu, P.-R.; Ji, M.-M.; Hu, J.-B.; Peng, J.-B. Manganese-catalyzed carbonylation of unactivated alkyl bromides with alkylidenecyclopropanes. *ACS Catal.* **2024**, 9487-9495.

(13) (a) Singh, S.; Chakraborty, G.; Raha Roy, S. Skeletal rearrangement through photocatalytic denitrogenation: access to C-3 aminoquinolin-2(1*H*)-ones. *Chem. Sci.* **2023**, *14*, 12541-12547. (b) Wu, X.; Zhang, X.; Ji, X.; Deng, G.-J.; Huang, H. Visible-light-induced cascade arylazidation of activated alkenes with trimethylsilyl azide. *Org. Lett.* **2023**, *25*, 5162-5167. (c) Zhu, Y.; Li, X.; Wang, X.; Huang, X.; Shen, T.; Zhang, Y.; Sun, X.; Zou, M.; Song, S.; Jiao, N. Silver-catalyzed decarboxylative azidation of aliphatic carboxylic acids. *Org. Lett.* **2015**, *17*, 4702-4705.

(14) Finkelstein, P.; Reisenbauer, J. C.; Botlik, B. B.; Green, O.; Florin, A.; Morandi, B. Nitrogen atom insertion into indenenes to access isoquinolines. *Chem. Sci.* **2023**, *14*, 2954-2959.

(15) Kaur, A.; Wang, S.; Yu, A.; Elrafei, T. N.; Steinberg, L.; Kumar, A. Real-world risk of anosmia with cancer directed systemic therapy: A pharmacovigilance assessment using FDA Adverse Events Reporting System (FAERS) database. *J. Clin. Oncol.* **2021**, *39*, e18790-e18790.

Acknowledgments

J.Z. gratefully acknowledges support from the National Natural Science Foundation of

China (52073141 and 22275083) and the Department of Science and Technology of
Jiangsu Province (BE2022839).